# Combining bioinformatics prediction with experimental validation to explore the ameliorative effect of *Psoralea corylifolia* on vitiligo

CHEN ZHANG[1], ZHANHONG CAO[1], MENGYANG WEI[1], XUANXUAN ZHU[1], YAN YAN[1], ZHENHUA WANG[2] and MENG ZHANG[1]

[1]College of Traditional Chinese Medicine, Bozhou University, Bozhou, Anhui 236800 P.R. China; [2]Anhui Shimao Traditional Chinese Medicine Co., Ltd., Bozhou, Anhui 236800, P.R. China

Received October 23, 2025; Accepted March 5, 2026

DOI: 10.3892/mmr.2026.13868

**Abstract.** The aim of the present study was to thoroughly examine the mechanism of action underlying the therapeutic efficacy of *Psoralea corylifolia* in the management of vitiligo, using a comprehensive approach integrating bioinformatics prediction with empirical validation. Network pharmacology and the GEO database were employed to construct a *P. corylifolia*-vitiligo-target network, screen the active ingredients of *P. corylifolia* and its core targets for vitiligo therapy, analyze target enrichment pathways, verify component-key target binding using molecular docking and validate using ultra-high-performance liquid chromatography-triple/time-of-flight mass spectrometry (UPLC-Q-TOF/MS), zebrafish and cellular experiments. The active ingredients of *P. corylifolia* used to treat diseases may include isobavachin, bavachin and stigmasterol, among others and the core targets may include AKT1, TNF, ESR1 and BCL2. The outcomes of the enrichment analysis predominantly pertained to signaling pathways, including apoptosis, protein phosphorylation, enzyme binding and pathways implicated in cancer and the PI3K-Akt signaling pathway. Molecular docking results indicated that core components exhibited low binding energies with key targets. UPLC-Q-TOF/MS analysis revealed that the main components of the aqueous and ethanol extracts of *P. corylifolia* included: Angelicin, psoralidin, stigmasterol, bavachin and bakuchiol. Experiments involving zebrafish and B16 melanocytes showed that the aqueous and ethanol extracts of *P. corylifolia* were able to increase melanin production. Within a certain range, greater concentrations resulted in greater melanin synthesis. The therapeutic effect of *P. corylifolia* in vitiligo treatment may be due to the active ingredients isobavachin, bavachin and stigmasterol, which act on Akt1, TNF and other targets and modulate apoptosis, protein phosphorylation and PI3K/Akt signaling pathways.

*Correspondence to:* Dr Meng Zhang, College of Traditional Chinese Medicine, Bozhou University, 668 Wencai Road, Bozhou, Anhui 236800, P.R. China
E-mail: 2024070013@bzuu.edu.cn

*Key words:* bioinformatics, *Psoralea corylifolia*, vitiligo, ultra-high-performance liquid chromatography-triple/time-of-flight mass spectrometry, zebrafish

## Introduction

Vitiligo is an acquired pigmentation disorder with a complex pathogenesis and a number of etiological factors. It is mainly manifested by limited or generalized depigmentation spots (1,2). Epidemiological investigations show that its incidence accounts for 1-2% of the total population and the total number of vitiligo patients in China is estimated to be 10-20 million. The incidence rate is increasing year on year and the average age of onset is decreasing (3). The etiology of vitiligo is complex and hypotheses have been proposed from various perspectives (4,5), including genetics, autoimmunity, oxidative stress, cytotoxicity and microenvironmental disorders. Currently, no single hypothesis fully explains the pathogenesis of vitiligo. However, it is clear that the final link in these hypotheses is the apoptosis or dysfunction of melanocytes (6).

The main treatments for vitiligo are non-pharmacological and pharmacological. Non-pharmacological treatments include melanocyte transplantation, iontophoresis and laser therapy, which have great limitations and are not a feasible treatment option for patients in the developmental stage and with large skin lesions (7). Pharmacological treatments for vitiligo mostly use high-dose glucocorticoids or immunosuppressants, which have significant side effects and produce unsatisfactory results. By contrast, in traditional Chinese medicine (TCM) the use of *Psoralea corylifolia (P. corylifolia)* is believed to tonify the kidneys, strengthen yang, and invigorate the spleen and stomach and it is widely used to treat psoriasis, vitiligo and a number of other dermatological conditions. *P. corylifolia* tincture is commonly used in the clinical treatment of vitiligo (8). However, further research is needed to elucidate its active ingredients, molecular targets and mechanisms of action.

Microarray analysis is a high-throughput method commonly used to explore the pathogenesis of human diseases. Bioinformatics are employed to analyze online microarray databases and identify key genes involved in disease development (9). The present study used bioinformatics to analyze the GSE75819 vitiligo-related microarray dataset in the

Gene Expression Omnibus (GEO) database. The aim was to explore the core genes involved in vitiligo occurrence and development and to provide a reference index for evaluating the therapeutic efficacy of *P. corylifolia* in vitiligo treatment. Network pharmacology is a new approach that can systematically and comprehensively analyze the mechanisms of drug action on disease by examining the interactions between active ingredients in TCM and disease targets (10), which can systematically and comprehensively explore the mechanisms of drug action on disease and coincides with the holistic and systematic view of TCM in treating diseases (11,12). Molecular docking technology, which is based on the principles of molecular mechanics and quantum mechanics, is used to predict the binding affinity of drugs and targets by calculating the energy changes between drug molecules and target proteins. In the present study, bioinformatics, network pharmacology and molecular docking were used to screen the main active ingredients of *P. corylifolia*, analyze the action targets and mechanisms of active ingredients and verify them through zebrafish and cell experiments. It not only provided theoretical foundation for the clinical application of *P. corylifolia* in the therapy of vitiligo, but also served as references for its further scientific research.

## Materials and methods

*Screening of medicinal chemical components and their targets*. The components of *P. corylifolia* that enter the bloodstream were obtained as potential active ingredients using the SymMap database (http://www.symmap.org/). The non-hemolytic constituents of psoralen were meticulously investigated within the TCMSP database (https://old.tcmsp-e.com/tcmsp.php) using the criteria of druglikeness ≥0.18 and oral bioavailability ≥30% as the selection parameters. The active ingredients obtained were searched for in the PubChem database (https://pubchem.ncbi.nlm.nih.gov/) to determine their chemical formulae. The Swiss Target Prediction tool (http://swisstargetprediction.ch/) was then used to determine the target of the active ingredient.

*GEO database and vitiligo target acquisition*. The GSE75819 (https://www.ncbi.nlm.nih.gov/geo/query/acc.cgi?acc=gse75819) transcriptome data (13), downloaded from the GEO database (http://www.ncbi.nlm.nih.gov/geo/), contains data from 15 vitiligo patients and 15 healthy individuals. Differential analysis was conducted using the 'limma' package (https://bioconductor.org/packages/release/bioc/html/limma.html) in the R programming language. Differential genes were identified using a significance level of $P<0.05$ and $|\log2FC|>1$ as the criteria. The findings were then depicted via volcano plots and heat maps to provide a comprehensive visualization. The differential genes and vitiligo genes from the GeneCards (https://www.genecards.org/) and DisGeNET databases (https://disgenet.com/) were brought together as vitiligo target genes using a Venn diagram (http://www.bioinformatics.com.cn). With the help of the online tool Venny 2.1.0 (http://liuxiaoyuyuan.cn/gongju/weientu.html), the vitiligo targets were intersected with the targets of the *P. corylifolia* active ingredient and the intersecting targets were identified as potential vitiligo interventions.

*Construction of the active ingredient-target-disease network*. Network and tape files consisting of *P. corylifolia* and its common targets with vitiligo were produced. These files were then be imported into Cytoscape 3.10.1 (https://apps.cytoscape.org/) application to construct the active ingredient-target-disease network.

*Construction of protein-protein interaction (PPI) networks and screening of core targets*. The possible targets of *P. corylifolia* for vitiligo were searched for in the STRING database (https://cn.string-db.org). Free nodes were eliminated and the resulting TSV files were downloaded, visualized and analyzed using Cytoscape 3.10.1.

*Gene Ontology (GO) and Kyoto Encyclopedia of Genes and Genomes (KEGG) pathway enrichment analysis*. GO and KEGG pathway data obtained from the intersecting genes of *P. corylifolia* and vitiligo were retrieved and downloaded with the help of the DAVID database (https://david.ncifcrf.gov). GO and KEGG enrichment analyses were conducted to investigate the biological pathways and potential functions of the intersecting genes, with the aim of analyzing their biological processes and metabolic pathways. Finally, the data were visualized using the MicroBioInformatics online tool (https://www. bioinformatics.com.cn).

*Molecular docking validation*. The 3D crystalline structure of the target protein was retrieved from the Protein Data Bank (PDB; https://www.rcsb.org/). It was then downloaded and processed for dehydration and hydrogenation using AutoDockTools (https://vina.scripps.edu/). This structure was ultimately selected as the receptor and preserved in the PDBqt file format. Active constituents were retrieved from the TCMSP database, hydrogenated using AutoDockTools and selected as ligands before being exported in the PDBQT file format. Molecular docking simulations were then performed using AutoDock Vina to determine the binding affinity of each compound to the target protein. Subsequent analysis of these affinities was conducted using the 'pheatmap' (https://cran.r-project.org/web/packages/pheatmap/index.html) and 'circlize' R packages (https://cran.r-project.org/web/packages/circlize/index.html), complemented by visualization in PyMOL (http://www.pymol.org/pymol).

*Preparation of aqueous and ethanol extracts*. *P. corylifolia* (10 g) was crushed and added to 100 ml of distilled water/75% ethanol. The mixture was left to soak for 1 h and then subjected to water bath heating extraction for a further 1 h. The extract was filtered and collected. Add a further 100 ml of distilled water/75% ethanol and perform a water bath heating extraction for a further 30 min. Filter and collect the extract, then combine the two extracts and concentrate them.

*Main materials and instruments*. AB wild-type zebrafish (Shanghai FishBio Co., Ltd.), B16F10 cells (Wuhan Pricella Biotechnology Co., Ltd.; Elabscience Bionovation Inc.), 3-(4,5-Dimethylthiazol-2-yl)-2,5-diphenyltetrazolium bromide; MTT; tetrazolium salt), N-phenylthiourea (PTU), levodopa (L-DOPA), laboratory biochemical incubator (Tianjin Laboratory Instrumentation Co., Ltd.), K-400L stereo

microscope (Motic Incorporation, Ltd.), SpectraMax iD3 multifunctional enzyme labeler (Molecular Devices, LLC.).

*Principal component analysis extract using ultra-high-performance liquid chromatography-triple/time-of-flight mass spectrometry (UPLC-Q-TOF/MS).* The aqueous and ethanol extracts of *P. corylifolia* were subjected to UPLC-Q-TOF/MS analysis to ascertain the total ion mobility map, in compliance with the chromatographic and mass spectrometric parameters as detailed in Tables SI and SII. Drawing upon the multistage mass spectrometric data derived from the samples, subsequent processing and comprehensive analysis were conducted in synergy with the high-resolution mass spectrometry database for natural products and pertinent scholarly literature.

*Establishment of a zebrafish model for pigment loss and drug experiments.* Preliminary experiments determined that 200 $\mu$M PTU would be used to generate a pigment-deficient zebrafish model. Zebrafish embryos were cultured in a constant-temperature incubator at 28˚C for 24 h, designated as 24hpf/1dpf. PTU-induced modeling was then performed for 48 h, at which point the embryos were designated as 72hpf/3dpf. Drug administration commenced immediately afterward for 72 h, with the final time point designated as 144hpf/6dpf. Experimental groups and procedures are detailed below: At 1 dpf, healthy zebrafish embryos were selected and placed into 6-well plates at 15 zebrafish embryos per well. Groups included: Blank control group cultured in fresh culture water; modelling group cultured in fresh culture water containing 200 $\mu$M PTU; and groups with different concentrations of aqueous and ethanol extracts (1, 2.5 and 5 $\mu$g/ml). Following drug administration, anesthesia was induced using 0.016% MS-222 until zebrafish ceased swimming or exhibited ventral positioning (flipping onto their backs), indicating full anesthesia (14). Anesthetized zebrafish were observed under a microscope within 5 min to assess pigment development, with images captured for documentation. After the experiment, zebrafish were immersed in a high-concentration 0.08% MS-222 solution (typically 5X) until gill movement ceased (~5 min). Anesthesia was maintained for an additional 10-15 min to ensure the mortality of experimental fish (15). Finally, they were placed in a -20˚C freezer for centralized disposal of all experimental animals (16). All zebrafish experiments were reviewed and approved by the Animal Ethics Committee of Bozhou University, with ethics approval number DFDW/BZUU-2025-ZF-031.

*Measurement of melanocyte viability.* B16F10 melanocytes in the exponential growth phase were carefully selected and inoculated into 96-well plates at a concentration of $5x10^4$ cells/ml in 180 $\mu$l of volume per well. Following inoculation, the cells were placed in a 5% $CO_2$ incubator at 37˚C and allowed to proliferate for 24 h. Subsequently, the cells were treated with aqueous and ethanol extracts of *P. corylifolia* at concentrations of 0.01, 0.1, 1, 10 and 100 $\mu$g/ml, followed by an incubation at 37˚C period of 48 h. The solution was then evacuated and discarded. Then, 30 $\mu$l of MTT reagent was added to each well and the reaction was carried out at 37˚C for 4 h. DMSO (150 $\mu$l) was added to each well and the solution was vigorously agitated for 10 min. After a 48-h incubation period, 30 $\mu$l of MTT reagent was added to each well. The reaction was then conducted at 37˚C for 4 h. Then, 150 $\mu$l of DMSO was added to each well and shaken for 10 min to facilitate the reaction. Absorbance readings for each well were taken at a wavelength of 570 nm to evaluate the effect of aqueous and alcoholic extracts derived from tonic acid on melanocyte viability and functional integrity.

*Determination of melanin content and tyrosinase activity of cells.* B16F10 melanocytes were cultured according to the procedure in the aforementioned *Measurement of melanocyte viability.* After 24 h, 0.01, 0.1, 1 and 10 $\mu$g/ml concentrations of the aqueous and ethanol extracts of *P. corylifolia* were added. After 72 h of incubation at 37˚C, the cells were washed twice with PBS, following which 100 $\mu$l of a non-denaturing lysis buffer containing 1 nM PMSF were added. The cells were lysed at 4˚C for a duration of 20 min, following which they were collected. Upon reaching 72 h of culture at 37˚C, the cells underwent a washing process with PBS, repeated twice. Thereafter, a volume of 100 $\mu$l of non-denaturing lysate, which contained 1 nM PMSF, was introduced. The cells were subsequently lysed once again at 4˚C for 20 min and then collected. The collected cells were centrifuged at 4˚C for 10 min at 21,756 x g. The resulting supernatant was used to determine the protein content via the BCA assay and the protein concentration was subsequently calculated. The volume of the supernatant containing 10 $\mu$g of total protein was measured and transferred to a 96-well plate. The volume was then brought up to 100 $\mu$l using PBS (0.1 M, pH 6.8). Then, 100 $\mu$l of a 0.01% L-DOPA solution was added and the plate was incubated at 37˚C in the dark for 3 h. OD475 was used to evaluate the catalytic activity of tyrosinase. The melanin precipitate pellet was then suspended in a 100 $\mu$l NaOH solution containing 10% DMSO to ensure full solubilization of the melanin within each experimental group. The melanin precipitate with the lower concentration was supplemented with 100 $\mu$l of a NaOH solution containing 10% DMSO. Then, 100 $\mu$l of the melanin solution was pipetted into each well of a 96-well plate. OD405 was determined to assess melanocyte content.

*Statistical analysis.* Data were analyzed exclusively using GraphPad Prism 5 software (Dotmatics), employing one-way analysis of variance (followed by Tukey's post hoc test) and two-tailed paired t-tests. $P<0.05$ was considered to indicate a statistically significant difference.

## Results

*Screening of the chemical constituents of P. corylifolia.* Searching the SymMap and TCMSP databases, the present study obtained nine constituents of *P. corylifolia*, including isobavachin, bavachin, stigmasterol, bavachalcone, bakuchiol, psoralidin and angelicin (Table I).

*Intersection of drug active ingredients and disease targets.* A total of 259 effective targets of the nine active components of *P. corylifolia* were obtained through the Swiss Target

Table I. Main active components of *Psoralea corylifolia*.

| CAS number | Active ingredient | Basis of selection |
|---|---|---|
| 31524-62-6 | Isobavachin | OB≥30%; DL≥0.18% |
| 19879-32-4 | Bavachin | Blood-entry component |
| 83-48-7 | Stigmasterol | OB≥30%; DL≥0.18% |
| 28448-85-3 | Bavachalcone | Blood-entry component |
| 10309-37-2 | Bakuchiol | Blood-entry component |
| 20784-50-3 | Isobavachalcone | Blood-entry component |
| 523-50-2 | Angelicin | Blood-entry component |
| 41743-38-8 | Bavachromene | Blood-entry component |
| 18642-23-4 | Psoralidin | Blood-entry component |

OB, oral bioavailability; DL, druglikeness.

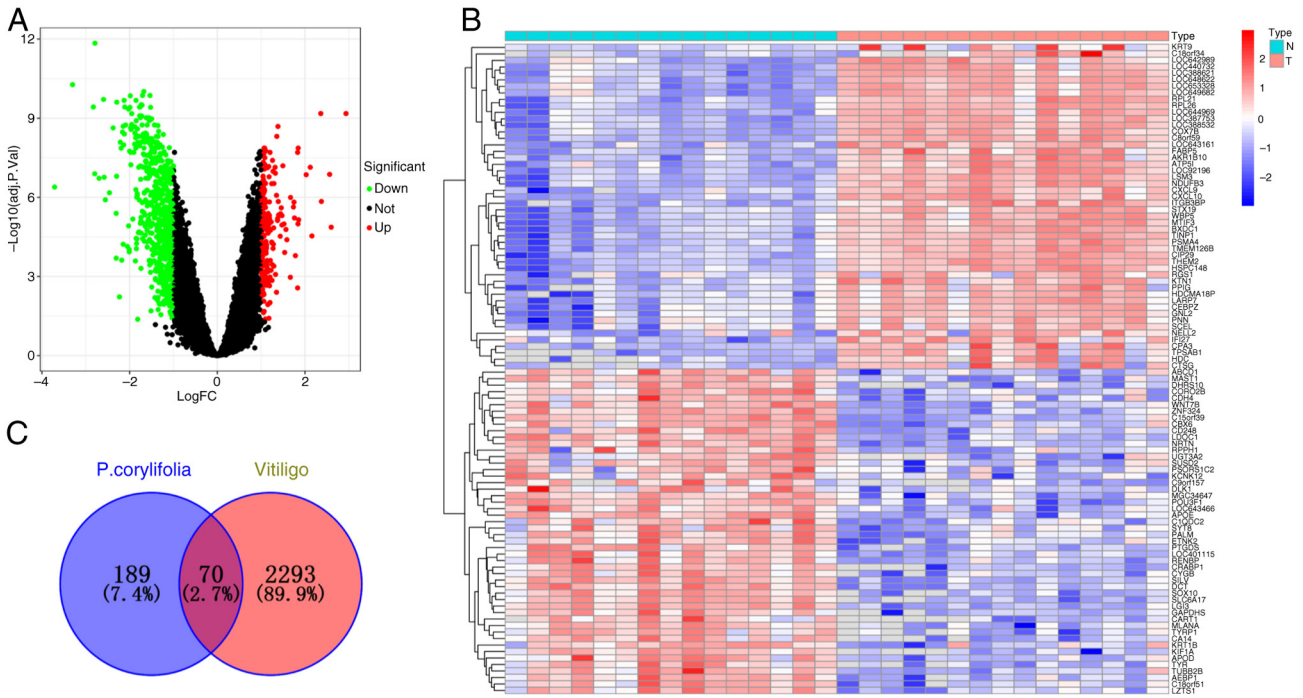


Figure 1. Drug active ingredient targets and disease targets. (A) DEGs volcano plot. (B) DEGs heat map. (C) Drug-disease target Venn diagram. DEGs, differentially expressed genes.

Prediction database. The GeneCards and DisGeNET databases screened 1,357 and 395 potential vitiligo targets, respectively. Microarray data from GSE75819 detected a total of 25,402 genes, including 691 upregulated and 220 downregulated genes (Fig. 1A and B). Using Venny, the intersection between the microarray differential genes related to vitiligo and the active ingredient targets of *P. corylifolia*, were identified obtaining a total of 70 intersecting genes (Fig. 1C). These included TNF, AKT1, PPARG, PTGS2, HSP90AA1, ESR1, BCL2, NFKB1, MTOR, GSK3B, PARP1, MDM2, MAPK1 and PIK3CA.

The Cytoscape 3.10.1 application was used to create the 'active ingredient-target-disease' network illustrated in Fig. 2A, comprising 80 nodes and 140 edges. The Network Analyzer, an integral component of the software, was used to calculate the degree value for each node. A higher degree value indicates a stronger association between the active components of *P. corylifolia* and vitiligo-related targets. The active ingredients of *P. corylifolia* based on degree value were isobavachin, bavachin, stigmasterol, bavachalcone, bakuchiol, isobavachalcone, psoralidin and angelicin, with degree values of 29, 26, 16, 16, 16, 13, 10 and 8, respectively. It suggested that these constituents may be crucial in the psoralen treatment of vitiligo.

*Construction of PPI network and screening of core targets.* The curated list of 70 intersecting genes was seamlessly integrated into the STRING database, giving rise to a sophisticated PPI network, specifically curated under the criterion of 'Homo sapiens'. This intricate network encompasses a total of 70 nodes interconnected by 461 edges, exhibiting an

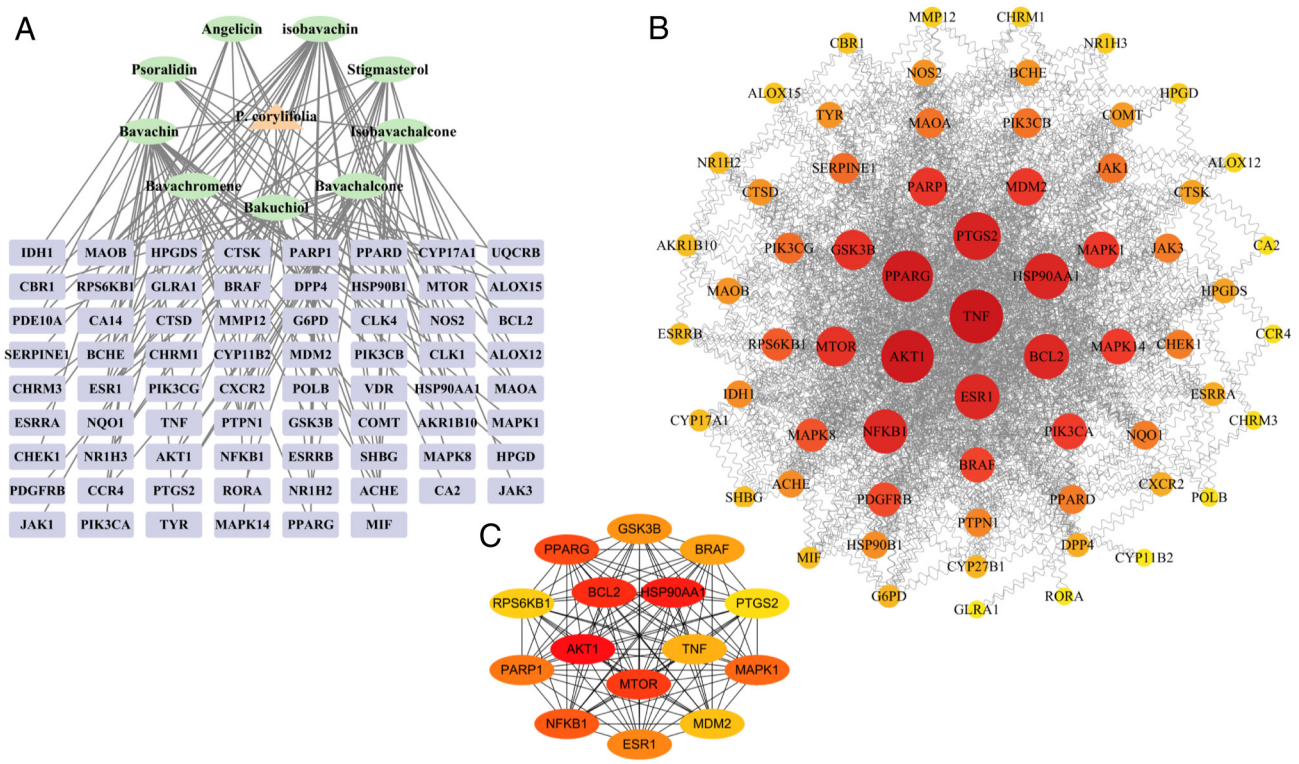


Figure 2. Construction of PPI network and screening of core targets. (A) Drug-target-gene network. (B) PPI diagram of potential targets for vitiligo treatment with *Psoralea corylifolia*. (C) Core target diagram of cytoHubba-MCC algorithm. PPI, protein-protein interaction.

average node degree of 13.2, as illustrated in Fig. 2B. The derived protein interaction data were meticulously integrated into the Cytoscape 3.10.1 software suite, wherein subsequent manipulation via the Analyze Network module facilitated the generation of an exhaustive network visualization. This visualization underscored the pivotal targets of *P. corylifolia* in the context of vitiligo therapeutic intervention, as depicted in Fig. 2B. In the figure the size of the circular node indicates the degree value, the larger node degree value, the redder node indicates that the target is more critical, the closer the relationship between the active ingredient of *P. corylifolia* and the target of vitiligo. The top 15 target proteins are TNF, AKT1, PPARG, PTGS2, HSP90AA1, ESR1, BCL2, NFKB1, MTOR, GSK3B, PARP1, MDM2, MAPK1, PIK3CA and MAPK14, with degree values of 86, 84, 80, 72, 68, 66, 66, 64, 54, 54, 50, 48, 46, 44, 44, respectively. The top 15 targets were further calculated by applying the MCC algorithm using the cytoHubba plug-in in Cytoscape software (Fig. 2C) and the intersection of the targets calculated by the MCC algorithm and Degree was taken to obtain a total of AKT1, HSP90AA1, BCL2, MTOR, NFKB1, MAPK1, ESR1, GSK3B, TNF, PTGS2 ten key targets. The identified targets may represent the principal therapeutic targets of *P. corylifolia* in the context of vitiligo treatment and they are concurrently the focus of molecular docking validation as presented in the present study.

*GO functional enrichment analysis*. The 70 overlapping genes were uploaded to the DAVID database for enrichment analysis, yielding results for 272 biological processes (BP), 41 cellular components (CC) and 66 molecular functions (MF). Following rigorous screening, the top ten candidates in each category were selected based on their P-values: BP, CC and MF. These selections were then depicted graphically via bar charts to facilitate a comprehensive visual comparison. The results showed that BP was mainly enriched in the regulation of apoptosis, protein phosphorylation and the inflammatory response; CC was mainly enriched in the mitochondria, the cytoplasm and the phosphatidylinositol 3-kinase complex; and MF was mainly enriched in homodimeric protein binding, enzyme binding and protein serine/threonine kinase activity, as shown in Fig. 3.

*KEGG pathway enrichment analysis*. The 70 intersecting genes obtained were imported into the DAVID database for enrichment analysis. The results of the enrichment analysis revealed 140 KEGG pathways and a KEGG functional enrichment bar graph was drawn according to the results of the top 20 P-values (Fig. 3B). The KEGG pathway enrichment results were categorized (Fig. 3C). The enrichment outcomes indicate that the genes are predominantly associated with multiple facets of the PI3K-Akt signaling pathway and oncogenic pathways, as well as pathways relevant to hepatitis.

*Results of molecular docking of core components and key targets*. The eight active ingredients of *P. corylifolia* obtained (Isobavachin, Bavachin, Stigmasterol, Bavachalcone, Bakuchiol, Isobavachalcone, Psoralidin and Angelicin) and the 10 key targets (AKT1, HSP90AA1, BCL2, MTOR, NFKB1, MAPK1, ESR1, GSK3B, TNF and PTGS2) were molecularly docked (Table II and Fig. 4A). The binding energy, measured in kilocalories per mole (kcal/mol), was found to

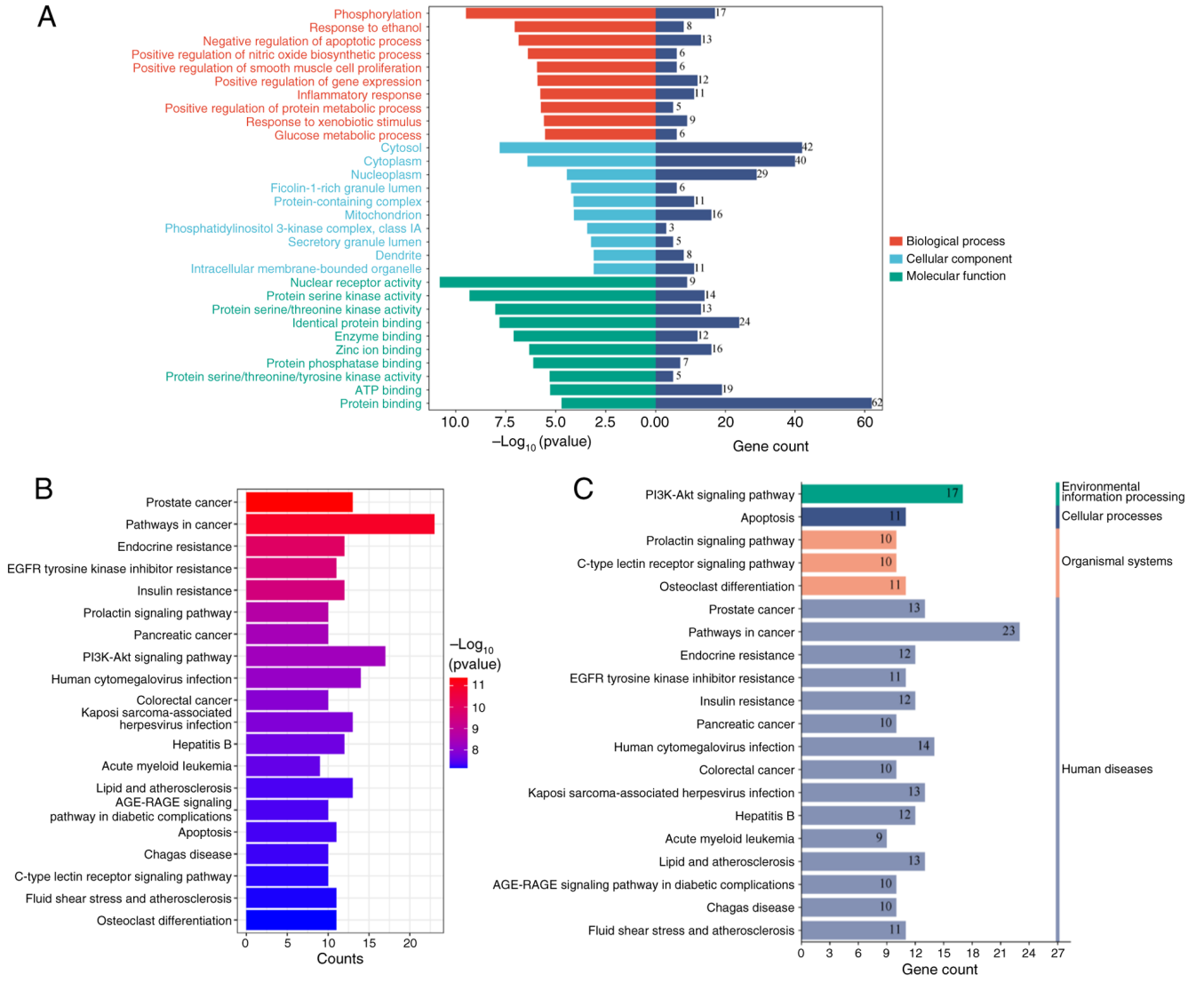


Figure 3. Analysis of GO enrichment and KEGG enrichment. The specific pathway of KEGG enrichment shown in the image comes from https://www.kegg.jp/kegg/pathway.html. (A) Bioprocesses enrichment, red: BP, blue: CC, green: MF. (B) KEGG enrichment. (C) KEGG Pathway enrichment. GO, Gene Ontology; KEGG, Kyoto Encyclopedia of Genes and Genomes; BP, biological processes; CC, cellular components; MF, molecular functions.

be <-5.0 kcal/mol, indicating a strong and stable interaction between the drug components and the key target proteins. It should be noted that a more negative binding energy denotes a stronger and more stable binding effect. The binding energy was found to be <-5.0 kcal/mol for all components, signifying robust and stable interactions with the key target proteins. The resultant binding energies for each constituent with respect to the target were visualized using a clustered heatmap generated via the 'pheatmap' R package (Fig. 4B).

*UPLC-Q-TOF/MS analysis of the main components of the aqueous and ethanol extracts of P. corylifolia*. UPLC-Q-TOF/MS analysis was employed to detect and comprehensively analyze the main components of the aqueous and ethanol extracts of *P. corylifolia*. UPLC-Q-TOF/MS technology was employed to detect and analyze the extracts and the results indicated that the main constituents in the aqueous and ethanolic extracts of *P. corylifolia* were angelicin, psoralidin, stigmasterol, bavachin and bakuchiol, among others (Fig. S1; Table III).

*Effect of the hydroalcoholic extract of P. corylifolia on pigment synthesis in normal and depigmented zebrafish*. Compared with the control group, the aqueous and ethanol extracts of *P. corylifolia* markedly affected pigment synthesis in depigmented zebrafish, with increased melanin synthesis as the administered drug concentration increased (Fig. 5).

*Effect of P. corylifolia hydroalcoholic extract on melanin synthesis*. Compared with the control group, the results revealed that 0.01-1 $\mu$g/ml of the aqueous and ethanol extracts of *P. corylifolia* had no effect on cell viability, 10 $\mu$g/ml promoted cell viability and 100 $\mu$g/ml markedly inhibited cell viability (Fig. 6A and D). Therefore, 0.01-1 $\mu$g/ml of the aqueous and ethanol extracts of *P. corylifolia* were selected for subsequent experiments on melanin synthesis and tyrosinase activity. Compared with the control group, 0.01-10 $\mu$g/ml of the aqueous extracts of *P. corylifolia* markedly promoted melanin synthesis, with the effect becoming more pronounced at concentrations of 0.01-1 $\mu$g/ml (Fig. 6B). Compared with the control group, 0.01 $\mu$g/ml of

Table II. Molecular docking results of core components and key targets.

| Targets | PDB-ID | Components | Binding energy, kcal/mol | RMSD (A) |
|---|---|---|---|---|
| AKT1 | 6NJS | Isobavachin | -6.5 | 4.329 |
| | | Bavachin | -6.7 | 1.989 |
| | | Stigmasterol | -6.0 | 2.927 |
| | | Bavachalcone | -6.0 | 2.029 |
| | | Bakuchiol | -5.2 | 1.395 |
| | | Isobavachalcone | -6.0 | 2.376 |
| | | Angelicin | -5.7 | 1.471 |
| | | Psoralidin | -6.9 | 1.293 |
| ESR1 | 2BJ4 | Isobavachin | -9.4 | 2.653 |
| | | Bavachin | -7.8 | 2.698 |
| | | Stigmasterol | -7.2 | 2.188 |
| | | Bavachalcone | -5.6 | 1.603 |
| | | Bakuchiol | -5.9 | 1.990 |
| | | Isobavachalcone | -6.7 | 2.369 |
| | | Angelicin | -5.4 | 3.204 |
| | | Psoralidin | -8.3 | 2.997 |
| GSK3B | 1H8F | Isobavachin | -8.4 | 2.412 |
| | | Bavachin | -8.9 | 2.995 |
| | | Stigmasterol | -6.1 | 4.803 |
| | | Bavachalcone | -6.1 | 3.931 |
| | | Bakuchiol | -6.3 | 2.064 |
| | | Isobavachalcone | -7.5 | 2.339 |
| | | Angelicin | -6.2 | 1.872 |
| | | Psoralidin | -9.7 | 2.737 |
| HSP90AA1 | 1AUE | Isobavachin | -6.9 | 1.491 |
| | | Bavachin | -6.9 | 1.860 |
| | | Stigmasterol | -7.3 | 1.534 |
| | | Bavachalcone | -5.7 | 1.506 |
| | | Bakuchiol | -5.2 | 1.905 |
| | | Isobavachalcone | -6.3 | 3.442 |
| | | Angelicin | -5.6 | 1.475 |
| | | Psoralidin | -8.0 | 1.910 |
| MAPK1 | 6D5Y | Isobavachin | -7.5 | 3.485 |
| | | Bavachin | -7.5 | 2.012 |
| | | Stigmasterol | -5.8 | 2.726 |
| | | Bavachalcone | -6.4 | 3.042 |
| | | Bakuchiol | -4.9 | 4.641 |
| | | Isobavachalcone | -7.3 | 3.702 |
| | | Angelicin | -6.2 | 2.500 |
| | | Psoralidin | -7.9 | 1.597 |
| BCL2 | 1G5M | Isobavachin | -7.0 | 2.448 |
| | | Bavachin | -7.9 | 1.519 |
| | | Stigmasterol | -5.9 | 4.630 |
| | | Bavachalcone | -5.5 | 4.418 |
| | | Bakuchiol | -3.9 | 1.915 |
| | | Isobavachalcone | -6.6 | 4.701 |
| | | Angelicin | -4.9 | 1.368 |
| | | Psoralidin | -8.0 | 1.939 |
| MTOR | 1AUE | Isobavachin | -8.6 | 2.072 |
| | | Bavachin | -8.3 | 2.156 |
| | | Stigmasterol | -7.3 | 1.819 |

Table II. Continued.

| Targets | PDB-ID | Components | Binding energy, kcal/mol | RMSD (A) |
|---|---|---|---|---|
| | | Bavachalcone | -5.8 | 3.613 |
| | | Bakuchiol | -3.6 | 2.333 |
| | | Isobavachalcone | -7.6 | 2.454 |
| | | Angelicin | -8.1 | 1.548 |
| | | Psoralidin | -8.8 | 1.722 |
| NFKB1 | 2DBF | Isobavachin | -6.1 | 2.756 |
| | | Bavachin | -6.2 | 2.643 |
| | | Stigmasterol | -4.9 | 3.402 |
| | | Bavachalcone | -5.2 | 3.792 |
| | | Bakuchiol | -4.4 | 2.338 |
| | | Isobavachalcone | -5.7 | 4.932 |
| | | Angelicin | -4.8 | 1.457 |
| | | Psoralidin | -7.7 | 1.939 |
| TNF | 4ZCH | Isobavachin | -8.2 | 2.607 |
| | | Bavachin | -7.7 | 1.316 |
| | | Stigmasterol | -5.1 | 3.696 |
| | | Bavachalcone | -6.3 | 1.544 |
| | | Bakuchiol | -5.0 | 5.426 |
| | | Isobavachalcone | -7.1 | 5.465 |
| | | Angelicin | -6.1 | 2.198 |
| | | Psoralidin | -8.8 | 1.990 |
| PTGS2 | 5F19 | Isobavachin | -9.2 | 3.501 |
| | | Bavachin | -9.9 | 3.245 |
| | | Stigmasterol | -7.4 | 2.953 |
| | | Bavachalcone | -7.2 | 2.932 |
| | | Bakuchiol | -4.9 | 3.905 |
| | | Isobavachalcone | -7.7 | 2.991 |
| | | Angelicin | -7.1 | 1.405 |
| | | Psoralidin | -10.7 | 1.006 |

RMSD ≤2 A, the conformational difference is very small and the result is perfect; 2 A<RMSD≤3 A, the conformational difference is small and the results are in the appropriate range; RMSD>3 A, the conformational difference is significant and the results are not reliable.

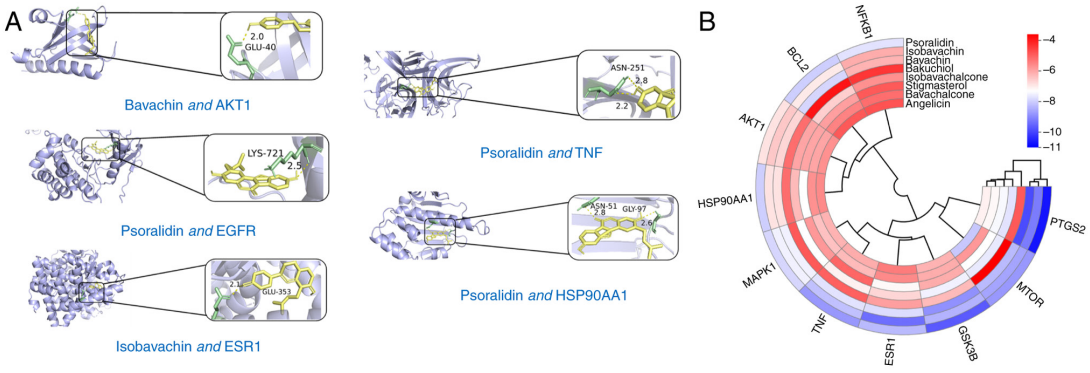


Figure 4. Molecular docking of core components with key targets. (A) Schematic diagram of molecular docking. (B) Heat map of binding energy clustering.

the ethanol extract of *P. corylifolia* had no significant effect on melanocyte synthesis, 0.1-10 $\mu$g/ml markedly promoted melanocyte melanin synthesis (Fig. 6E). Compared with the control group, 0.1-10 $\mu$g/ml of the aqueous extract markedly increased tyrosinase activity, with a more pronounced effect at higher concentrations (Fig. 6C and F).

Table III. Identification of the main components of *Psoralea corylifolia* extract samples.

| Serial no. | m/z | Molecular formula | Main components | Aqueous extract | | Ethanol extract | |
|---|---|---|---|---|---|---|---|
| | | | | Time/min | Peak area | Time/min | Peak area |
| 1 | 187.0386 | $C_{11}H_6O_3$ | Isopsoralen | 58.946 | 1,51,577 | - | - |
| 2 | 273.1835 | $C_{18}H_{24}O_2$ | Bakuchiol | 65.861 | 8,76,676 | 65.857 | 881.293 |
| 3 | 893.7206 | $C_{57}H_{96}O_7$ | 2-Glc-Stigmasterol | 66.618 | 1,55,60,238 | 10.187 | 15.560.238 |
| 4 | 187.0395 | $C_{11}H_6O_3$ | Psoralen | 1.402 | 5,77,113 | 63.182 | 880.119 |
| 5 | 325.1428 | $C_{20}H_{20}O_4$ | Bavachin | - | - | 0.9 | 48.755 |
| 6 | 339.1586 | $C_{20}H_{20}O_4$ | Bavachinin | 2.106 | 2,90,604 | - | - |

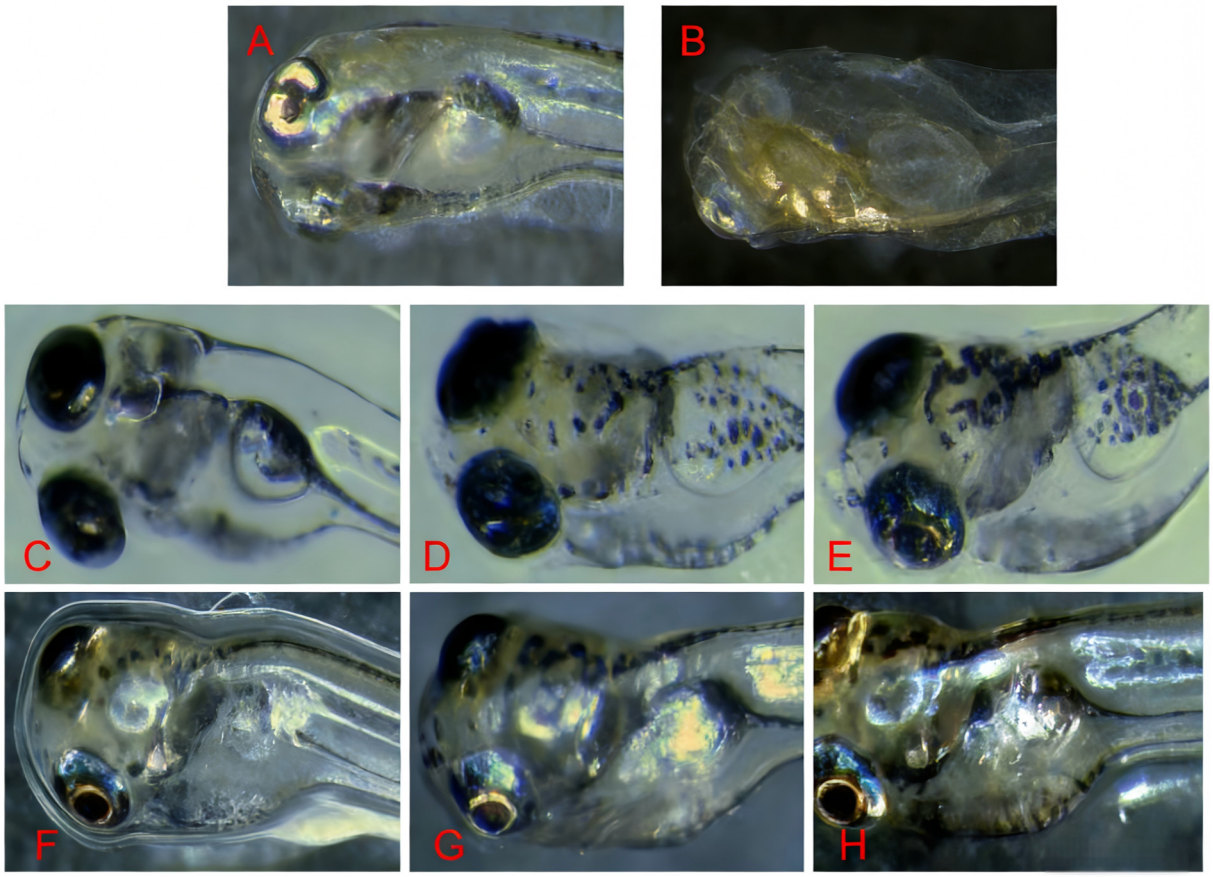


Figure 5. Effects of extracts of *Psoralea corylifolia* on pigment synthesis in normal and depigmented zebrafish. (A) Control. (B) N-phenylthiourea. Aqueous extract of *Psoralea corylifolia* (C) 1 μg/ml, (D) 2.5 μg/ml and (E) 5 μg/ml. Ethanol extracts of *Psoralea corylifolia* (F) 1 μg/ml, (G) 2.5 μg/ml and (H) 5 μg/ml.

## Discussion

A thorough search of the SymMap and TCMSP databases in the current investigation revealed that the primary active constituents of *P. corylifolia* that are effective in the treatment of vitiligo potentially include isobavachin, bavachin, stigmasterol, bavachalcone, bakuchiol, psoralidin and angelicin. Principal component analysis using UPLC-Q-TOF/MS showed that the aqueous and ethanol extracts of *P. corylifolia* contain these active ingredients. The phytochemicals isobavachin, bavachin, angelicin and stigmasterol have pharmacological properties including anti-inflammatory and antioxidant effects (17,18). Bavachalcone has the ability to modulate the NF-κB signaling pathway, effectively suppressing the synthesis of pro-inflammatory cytokines and demonstrating its anti-inflammatory properties (19). Melanocyte damage caused by free radicals induced by ultraviolet light and sunlight exposure is one of the main causes of vitiligo exacerbation, so antioxidant and free radical scavenging properties are important for curing vitiligo. Bakuchiol can scavenge oxidized free radicals and inhibit the production of interleukin-6 in various cell lines, exhibiting antioxidant and anti-inflammatory properties (20). It has

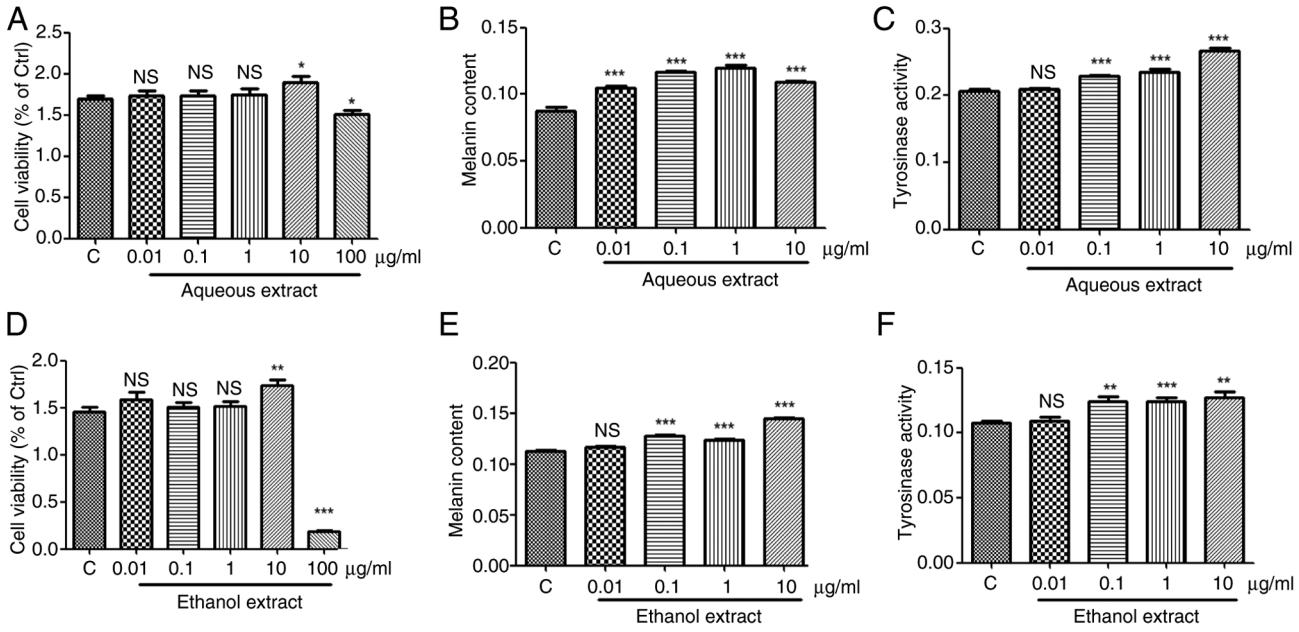


Figure 6. Effect of different concentrations of aqueous and ethanol extracts of *Psoralea corylifolia* on melanocyte viability, melanin content and tyrosinase activity. (A and D) Cell viability. (B and E) Melanin content. (C and F) Tyrosinase activity. NS, P>0.05; $^{*}$P<0.05; $^{**}$P<0.01; $^{***}$P<0.001.

been demonstrated that psoralidin activates tyrosinase, the rate-limiting enzyme in melanogenesis, conferring therapeutic efficacy against vitiligo (21). This suggests that the treatment of vitiligo with *P. corylifolia* is due to the combined effect of its active ingredients.

The establishment of the PPI network and the outcomes of the topological analysis conducted in the present study revealed that the key targets of *P. corylifolia* in its anti-vitiligo effects include AKT1, HSP90AA1, BCL2, MTOR, NFKB1, MAPK1, ESR1, GSK3B, TNF and PTGS2. AKT serves as a critical junction within the signaling cascade of protein kinase B and also plays a pivotal role in the organism's protein metabolic processes (22). At the same time, activated AKT1 mainly induces downstream signaling cascades by phosphorylating substrate proteins and participates in regulating various cellular activities (23,24), thereby adjusting the decline in autoimmune function due to vitiligo disease. TNF is a large group of cytokines that can directly cause tumor cell death. The present study identifies TNF-α, primarily produced by monocyte macrophages, as a key pro-inflammatory and immunomodulatory factor. Not only does it suppress the proliferation and differentiation of hematopoietic cells, inducing apoptosis, it also mitigates skin inflammation associated with vitiligo and enhances the immune response of the body (25). PTGS2, also known as cyclooxygenase, is a key prostaglandin endoperoxide synthase. It is a key enzyme in the metabolism of arachidonic acid to generate prostaglandins and is widely distributed in the body. When cells are stimulated, the expression of PTGS2 is increased and it catalyzes the production of various prostaglandins from arachidonic acid. These prostaglandins produce therapeutic effects such as pain relief, an anti-inflammatory response and anti-fibrosis. Prostaglandins are produced by keratinocyte-forming cells under ultraviolet irradiation and can promote melanocyte proliferation, dendrite growth and melanin production. This can treat skin melanin loss caused by vitiligo (26) and suggests that treating vitiligo with *P. corylifolia* is effective.

The findings of the present study suggested that the therapeutic mechanisms of *P. corylifolia* in the treatment of vitiligo involved the PI3K/AKT signaling pathway, oncological pathways and hepatitis-associated pathways. Vitiligo, cancer and hepatitis exhibit significant commonalities at the molecular pathway level, with their core mechanisms converging in three areas: Immune dysregulation, abnormal activation of key signaling pathways and oxidative stress damage. Research indicates that all three conditions rely on $CD8^{+}$ T cell-mediated cytotoxic responses, whereby perforin and granzyme are released to disrupt the membrane integrity of target cells (melanocytes, hepatocytes or tumor cells), thereby inducing cellular dysfunction or death (27-29).

Concurrently, sustained activation of the IFN-γ/JAK-STAT pathway serves as a central pro-inflammatory driver. By binding to IFNGR1/2 receptors, it induces STAT1 phosphorylation and nuclear translocation, thereby regulating hundreds of pro-inflammatory genes and exacerbating tissue damage. This pathway promotes melanocyte clearance in vitiligo, amplifies antiviral inflammatory responses in hepatitis and plays dual roles in antitumor immune responses and immune editing in cancer (30-32). Shared signaling networks (such as NF-κB, PI3K-AKT and MAPK) further link the pathologies of these three conditions. NF-κB forms a positive feedback inflammatory loop via TLR/IL-1R activation, driving the release of proinflammatory factors (TNF-α and IL-6); the PI3K-AKT pathway suppresses melanocyte survival signaling in vitiligo, but promotes tumor metabolic reprogramming in cancer (33); and MAPK mediates neuropeptide (CGRP)-induced immune activation in vitiligo and proinflammatory signaling from viral proteins (such as HBx) in hepatitis (34). The synergistic effects of oxidative stress create a vicious 'inflammation-oxidative stress' cycle through the excessive accumulation of reactive

oxygen species. Sources include melanin synthesis by-products (vitiligo), mitochondrial dysfunction (cancer) and viral protein-induced endoplasmic reticulum stress (hepatitis), ultimately leading to cellular dysfunction or malignant transformation (35).

Zebrafish have a number of advantages in melanin-related studies (36,37): i) Their transparent embryos enable real-time visualization of melanocyte development and migration; ii) their melanogenesis pathways are highly conserved with those of mammals; iii) they enable high-throughput screening for genetic and pharmacological interventions; and iv) they provide a more cost-effective alternative to mammalian models while maintaining biological relevance. In addition, the B16F10 cell line is a melanoma cell line that is also widely used and recognized in research related to pigmentation, including melanin formation, melanocyte biology and studies on potential interventions for pigmentary disorders such as vitiligo (38,39). The experimental results of the present study show that the aqueous and ethanol extracts of *P. corylifolia* can increase melanin production in zebrafish and B16 melanocytes. Within a certain range, the higher the concentration, the greater the melanin synthesis, which plays a role in curing vitiligo. This is because *P. corylifolia* can effectively enhance the proliferation rate of melanocytes and keratinocytes, promote melanocytes to enter the S and $G_2$ phases of the cell cycle and increase their division and proliferation. It can also enhance the activity of tyrosinase, a key enzyme in vitiligo treatment, ultimately leading to a significant increase in melanin synthesis (40). Further investigations have revealed that isobavachin acts as an anti-inflammatory modulator that effectively inhibits inflammatory responses *in vitro* and *in vivo* by modulating the MAPK and NF-κB signaling pathways. This suggests that isobavachin may exert therapeutic efficacy against vitiligo via its anti-inflammatory properties (16). Stigmasterol is a novel inhibitor of Nrf2, a 'master regulator' of the antioxidant response which reduces Nrf2 protein levels (41). The compromised Nrf2 pathway in melanocytes from vitiligo patients reduces the activation of the antioxidant enzyme system, resulting in dysregulated cellular autophagy. This, in turn, increases the sensitivity of vitiligo melanocytes to oxidative stress, thereby facilitating the onset and progression of vitiligo (42). Therefore, it was hypothesized that *P. corylifolia* exerts its therapeutic effects on vitiligo through multiple active ingredients acting on key targets along multiple pathways. Further refinement of quantitative assays for melanin production in zebrafish remains necessary. Additionally, validation of the targets and pathways implicated in the present study should be conducted in primary melanocytes and vitiligo animal models using approaches such as target fishing and gene silencing (short interfering/small hairpin RNA).

*P. corylifolia* may exert its effects through active ingredients such as isobavachin, bavachin and stigmasterol, which act on core targets such as AKT1, BCL2 and MAPK1 and affect signaling pathways such as PI3K/AKT, thereby treating vitiligo. The current study provided a conceptual basis for the use of *P. corylifolia* in the prophylaxis and therapy of vitiligo, although the intricacies of its pharmacodynamic mechanism require further investigation.

**Acknowledgements**

Not applicable.

**Funding**

The present study was supported by 2023 Anhui Province Higher Education Science Research Project (grant nos. 2023AH052279 and 2023AH052272) and 2024 Bozhou College Horizontal Project (grant nos. BYH202485, BYH2025016 and BYH2025098).

**Availability of data and materials**

The data generated in the present study may be requested from the corresponding author.

**Authors' contributions**

MZ and CZ conceived and supervised the project and designed the experiments. CZ, MZ, XZ, MW, ZW, ZC and YY collected the data. CZ, ZW and XZ analyzed the data. CZ drafted the manuscript. XZ and CZ confirm the authenticity of all the raw data. All authors contributed to manuscript revision. All authors have read and approved the final manuscript.

**Ethics approval and consent to participate**

All zebrafish experiments were reviewed and approved by the Animal Ethics Committee of Bozhou University, with ethics approval number DFDW/BZUU-2025-ZF-031.

**Patient consent for publication**

Not applicable.

**Competing interests**

The authors declare that they have no competing interests.

**References**

1. Frisoli ML, Essien K and Harris JE: Vitiligo: Mechanisms of pathogenesis and treatment. Annu Rev Immunol 38: 621-648, 2020.
2. Araj S, Kemp EH and Gawkrodger DJ: Pathoimmunological mechanisms of vitiligo: The role of the innate and adaptive immunities and environmental stress factors. Clin Exp Immunol 207: 27-43, 2022.
3. Tong XY, Wang Y, Duan C, Jia H, Wei MY and Chang XT: Clinical epidemiologic analysis of 112 cases of vitiligo in children. Dermatol Venereol 42: 875-876, 2020.
4. Faraj S, Kemp EH and Gawkrodger DJ: Patho-immunological mechanisms of vitiligo: the role of the innate and adaptive immunities and environmental stress factors. Clin Exp Immunol 207: 27-43, 2022.
5. Marchioro HZ, Silva de Castro CC, Fava VM, Sakiyama PH, Dellatorre G and Miot HA: Update on the pathogenesis of vitiligo. An Bras Dermatol 97: 478-490, 2022.
6. Chen J, Li S and Li C: Mechanisms of melanocyte death in vitiligo. Med Res Rev 41: 1138-1166, 2021.
7. Wade-Irimada M, Tsuchiyama K, SasakiI R, Hatchome N, Watabe A, Kimura Y, Yamasaki K and Aiba S: Efficacy and safety of i.v. methylprednisolone pulse therapy for vitiligo: A retrospective study of 58 therapy experiences for 33 vitiligo patients. J Dermatol 48: 1090-1093, 2021.

8. Shi N, Chen Y, Wang J and Ni H: Clinical observation on the effect of Zengse Pill in treating patients with vitiligo of qi-stagnancy and blood-stasis syndrome type. Chin J Integr Med 14: 303-306, 2008.
9. Wang K, Guan C, Shang X, Ying X, Mei S, Zhu H, Xia L and Chai Z: A bioinformatic analysis: The overexpression and clinical significance of FCGBP in ovarian cancer. Aging (Albany NY) 13: 7416-7429, 2021.
10. He D, Huang JH, Zhang ZY, Du Q, Peng WJ, Yu R, Zhang SF, Zhang SH and Qin YH: A network pharmacology-based strategy for predicting active ingredients and potential targets of LiuWei DiHuang pill in treating type 2 diabetes mellitus. Drug Des Devel Ther 13: 3989-4005, 2019.
11. Li Y, Yang Q and Yu Y: A network pharmacological approach to investigate the mechanism of action of active ingredients of *Epimedii Herba* and their potential targets in treatment of Alzheimer's disease. Med Sci Monit 26: e926295, 2020.
12. Chen S, Jiang H, Cao Y, Wang Y, Hu Z, Zhu Z and Chai Y: Drug target identification using network analysis: Taking active components in Sini decoction as an example. Sci Rep 6: 24245, 2016.
13. Singh A, Gotherwal V, Junni P, Vijayan V, Tiwari M, Ganju P, Kumar A, Sharma P, Fatima T, Gupta A, *et al*: Mapping architectural and transcriptional alterations in non-lesional and lesional epidermis in vitiligo. Sci Rep 7: 9860, 2017.
14. Katz EM, Chu DK, Casey KM, Jampachaisri K, Felt SA and Pacharinsak C: The stability and efficacy of tricaine methanesulfonate (MS222) solution after long-term storage. J Am Assoc Lab Anim Sci 59: 393-400, 2020.
15. Matthews M and Varga ZM: Anesthesia and euthanasia in zebrafish. ILAR J 53: 192-204, 2021.
16. Wallace CK, Bright LA, Marx JO Andersen RP, Mullins MC and Carty AJ: Effectiveness of rapid cooling as a method of euthanasia for young zebrafish (Danio rerio). J Am Assoc Lab Anim Sci 57: 58-63, 2018.
17. Chung YC, Song SJ, Lee A, Jang CH, Kim CS and Hwang YH: Isobavachin, a main bioavailable compound in psoraleae fructus, alleviates lipopolysaccharide-induced inflammatory responses in macrophages and zebrafish by suppressing the MAPK and NF-κB signaling pathways. J Ethnopharmacol 321: 117501, 2024.
18. Park J, Seo E and Jun HS: Bavachin alleviates diabetic nephropathy in db/db mice by inhibition of oxidative stress and improvement of mitochondria function. Biomed Pharmacother 161: 114479, 2023.
19. Wu X, Zhang Z, Zhang X, Guo YP, Liu F, Gong JW, Li L, Chen XY and Li ZP: Upregulation of A20 and TAX1BP1 contributes to the anti-neuroinflammatory and antidepressant effects of bavachalcone. Int Immunopharmacol 122: 110552, 2023.
20. Nizam NN, Mahmud S, Ark SA, Kamruzzaman M and Hasan M: Bakuchiol, a natural constituent and its pharmacological benefits. F1000Res 12: 29, 2023.
21. Shi M, Zhang Y, Song M, Sun Y, Li C and Kang W: Screening the marker components in *Psoralea corylifolia* L. with the aids of Spectrum-effect relationship and component Knock-Out by UPLC-MS$^2$. Int J Mol Sci 19: 3439, 2018.
22. Basnet R and Basnet BB: Overview of protein kinase B enzyme: A potential target for breast and prostate cancer. Curr Mol Pharmacol 14: 527-536, 2021.
23. Balasuriya N, McKenna MS, Liu XG, Li S and O'donoghue P: Phosphorylation-dependent inhibition of Akt1. Genes (Basel) 9: 450, 2018
24. Kim MY, Park JY and Park HS: Akt1-mediated phosphorylation of RBP-Jk controls notch1 signaling. Biochemistry (Moscow) 84: 1537-1546, 2019.
25. Li W, Liu Q, Shi J, Xu X and Xu J: The role of TNF-α in the fate regulation and functional reprogramming of mesenchymal stem cells in an inflammatory microenvironment. Front Immunol 14: 1074863, 2023.
26. Fang P, Han Y, Qu Y, Wang X, Zhang Y, Zhang W, Zhang N, Li G and Ma W: EIF3B stabilizes PTGS2 expression by counteracting MDM2-mediated ubiquitination to promote the development and progression of malignant melanoma. Cancer Sci 113: 4181-4192, 2022.
27. Chang Y, Kang P, Cui T, Guo W, Zhang W, Du P, Yi X, Guo S, Gao T, Li C and Li S: Pharmacological inhibition of demethylzeylasteral on JAK-STAT signaling ameliorates vitiligo. J Transl Med 21: 434, 2023.
28. Zimmerer JM, Ringwald BA, Chaudhari SR, Han J, Peterson CM, Warren RT, Hart MM, Abdel-Rasoul M and Bumgardner GL Invariant NKT cells promote the development of highly cytotoxic multipotent CXCR3+CCR4+CD8+ T cells that mediate rapid hepatocyte allograft Rejection. J Immunol 207: 3107-3121, 2021.
29. Deo AS, Sruthika SU, Karun S, Bisaria K and Sarkar K: Participation of T cells in generating immune protection against cancers. Pathol Res Pract 262: 155534, 2024.
30. Li C, Wang W, Shao J, Zhou S, Ji X, Xi Y, Xu Q, Huang Y, Wang J, Wan Y and Li Z: Biomimetic polydopamine loaded with Janus kinase inhibitor for synergistic vitiligo therapy via hydrogel microneedles. J Nanobiotechnology 23: 63, 2025.
31. Ezeonwumelu IJ, Garcia-Vidal E and Ballana E: JAK-STAT pathway: A novel target to tackle viral infections. Viruses 13: 2379, 2021.
32. Jia JJ, Zhou X and Chu Q: Mechanisms and therapeutic prospect of the JAK-STAT signaling pathway in liver cancer. Mol Cell Biochem 480: 1-17, 2025.
33. Teng Y, Fan Y, Ma J, Lu W, Liu N, Chen Y, Pan W and Tao X: The PI3K/Akt pathway: Emerging roles in skin homeostasis and a group of non-malignant skin disorders. Cells 10: 1219, 2021.
34. Liu T, Xi T, Dong X and Xu D: Research progress on pathogenesis of skin pigmentation in chronic liver disease. Biomol Biomed 25: 1218, 2024.
35. Chaudhari N, Talwar P, Parimisetty A, Hellencourt CL and Ravanan P: A molecular web: Endoplasmic reticulum stress, inflammation, and oxidative stress. Front Cell Neurosci 8: 213, 2014.
36. Suo LH, Hou FY, Wang ZY, Wu CH, Xie J, Miao WG, Fan YM and Zhang J: Spirodiclofen inhibited melanin synthesis in zebrafish embryos. Pestic Biochem Physiol 210: 106397, 2025.
37. Ferreira AM, de Souza AA, Koga RCR, Sena IDS, Matos MJS, Tomazi R, Ferreira IM and Carvalho JCT: Anti-melanogenic potential of natural and synthetic substances: Application in zebrafish model. Molecules 28: 1053, 2023.
38. Khongkarat P, Kitipaspallop W, Puthong S, Pimtong W, Phuwapraisirisan P and Chanchao C: The in cellular and in vivo melanogenesis inhibitory activity of safflospermidines from *Helianthus annuus* L. bee pollen in B16F10 murine melanoma cells and zebrafish embryos. PLoS One 20: e0325264, 2025.
39. Wusiman Z, Zhang AM, Zhang SS, Zhao PP, Kang YT, Zhang Y, Li ZJ and Huo SX: Galangin ameliorates PTU-induced vitiligo in zebrafish and B16F10 cells by increasing melanogenesis through activation of the p38/JNK MAPK pathway. Front Pharmacol 16: 1521097, 2025.
40. Chen L, Chen S, Li P, Zhao X, Sun P, Liu X, Wei H, Jiang X, Zhan Z and Wang J: Exploration of the mechanism of Qinglongyi-Buguzhi drug pair in treating vitiligo based on network pharmacology, molecular docking and experimental verification. J Ethnopharmacol 334: 118595, 2024.
41. Liao H, Zhu D, Bai M, Chen H, Yan S, Yu J, Zhu H, Zheng W and Fan G: Stigmasterol sensitizes endometrial cancer cells to chemotherapy by repressing Nrf2 signal pathway. Cancer Cell Int 20: 480, 2020.
42. Lin X, Meng X, Song Z and Lin J: Nuclear factor erythroid 2-related factor 2 (Nrf2) as a potential therapeutic target for vitiligo. Arch Biochem Biophys 696: 108670, 2020.